

ORIGINAL ARTICLE

IncRsp1, a long noncoding RNA, influences *Fgsp1* expression and sexual reproduction in *Fusarium graminearum*

Jie Wang^{1,2} | Wenping Zeng^{1,3} | Jiasen Cheng^{1,2}  | Jiatao Xie^{1,2} | Yanping Fu² | Daohong Jiang^{1,2} | Yang Lin² 

¹State Key Laboratory of Agricultural Microbiology, Huazhong Agricultural University, Wuhan, China

²Hubei Key Laboratory of Plant Pathology, Huazhong Agricultural University, Wuhan, China

³Key Laboratory of Environment Change and Resources Use in Beibu Gulf, Ministry of Education, Nanning Normal University, Nanning, China

Correspondence

Yang Lin, Hubei Key Laboratory of Plant Pathology, Huazhong Agricultural University, Wuhan 430070, China.
Email: yanglin@mail.hzau.edu.cn

Funding information

National Natural Science Foundation of China, Grant/Award Number: 31301614 and 31901840

Abstract

Long noncoding RNAs (lncRNAs) are crucial regulators of gene expression in many biological processes, but their biological functions remain largely unknown, especially in fungi. *Fusarium graminearum* is an important pathogen that causes the destructive disease Fusarium head blight (FHB) or head scab disease on wheat and barley. In our previous RNA sequencing (RNA-Seq) study, we discovered that *IncRsp1* is an lncRNA that is located +99 bp upstream of a putative sugar transporter gene, *Fgsp1*, with the same transcription direction. Functional studies revealed that $\Delta IncRsp1$ and $\Delta Fgsp1$ were normal in growth and conidiation but had defects in ascospore discharge and virulence on wheat coleoptiles. Moreover, *IncRsp1* and *Fgsp1* were shown to negatively regulate the expression of several deoxynivalenol (DON) biosynthesis genes, *TRI4*, *TRI5*, *TRI6*, and *TRI13*, as well as DON production. Further analysis showed that the overexpression of *IncRsp1* enhanced the ability of ascospore release and increased the mRNA expression level of the *Fgsp1* gene, while *IncRsp1*-silenced strains reduced ascospore discharge and inhibited *Fgsp1* expression during the sexual reproduction stage. In addition, the *IncRsp1* complementary strains *IncRsp1-LC-1* and *IncRsp1-LC-2* restored ascospore discharge to the level of the wild-type strain PH-1. Taken together, our results reveal the distinct and specific functions of *IncRsp1* and *Fgsp1* in *F. graminearum* and principally demonstrate that *IncRsp1* can affect the release of ascospores by regulating the expression of *Fgsp1*.

KEYWORDS

DON production, *Fgsp1*, *Fusarium graminearum*, long noncoding RNA, sexual reproduction

1 | INTRODUCTION

The regulatory roles of long noncoding RNAs (lncRNAs) have been well described in animals, plants, and fungi, where they serve as crucial regulators of transcription in a wide range of biological processes (Ponting et al., 2009; Rinn et al., 2007; Swiezewski et al., 2009; Yamashita et al., 2016). lncRNAs can participate in controlling

gene expression via various molecular mechanisms. For example, the *DHFR* (human dihydrofolate reductase) gene contains two promoters. The minor promoter upstream of *DHFR* encodes an lncRNA that forms a triplex structure with the sequences of the major promoter and interacts directly with transcription factor IIB (TFIIB), resulting in the dissociation of the transcription initiation complex from the major promoter and inhibitor of *DHFR* (Martianov et al., 2007; Quan

This is an open access article under the terms of the Creative Commons Attribution-NonCommercial-NoDerivs License, which permits use and distribution in any medium, provided the original work is properly cited, the use is non-commercial and no modifications or adaptations are made.

© 2021 The Authors. *Molecular Plant Pathology* published by British Society for Plant Pathology and John Wiley & Sons Ltd.

et al., 2015). *COLD AIR*, an *Arabidopsis* intronic lncRNA induced by cold treatment, has been shown to recruit Polycomb Repressive Complex 2 (PRC2) to suppress the *FLOWER LOCUS C (FLC)* after vernalization (Heo & Sung, 2011). *Saccharomyces cerevisiae SER3* is involved in serine biosynthesis, the 3' end of lncRNA *SRG1* overlaps with the promoter of *SER3*, and the elongation of *SRG1* inhibits the initiation of *SER3* transcription by transcription interference under serine-rich conditions (Martens et al., 2004).

In recent years, several studies have identified or predicted the lncRNAs involved in the growth and development of filamentous fungi such as *Neurospora crassa* (Arthanari et al., 2014; Cemel et al., 2017), *Ustilago maydis* (Donaldson & Saville, 2013; Ostrowski & Saville, 2017), *Fusarium graminearum* (Kim et al., 2018; Wang et al., 2021), *Trichoderma reesei* (Till, Pucher, et al., 2018), and *Ustilaginoidea virens* (Tang et al., 2021). However, there are only a few surveys regarding the functional identification of lncRNAs in filamentous fungi. One of the best known lncRNAs is *qrf* in *N. crassa*. *qrf* is a long noncoding antisense RNA of the circadian clock core regulatory *frq* gene and inhibits the expression of *frq* by mediating chromatin modification (Belden et al., 2011; Li et al., 2015; Xue et al., 2014). The lncRNA *HAX1* interacts with a transcriptional activator Xylanase regulator 1 (*Xyr1*), interferes with the negative feedback regulatory loop of *Xyr1*, and ultimately promotes cellulase expression and activity in *T. reesei* (Till, Mach, et al., 2018; Till, Pucher, et al., 2018). Our recent studies suggest that a novel antisense lncRNA, *GzmetE-AS*, is involved in asexual and sexual reproduction by regulating its antisense gene *GzmetE* through the RNAi pathway in *F. graminearum* (Wang et al., 2021). These data reveal that lncRNAs also play important regulatory roles in filamentous fungi.

F. graminearum (teleomorph *Gibberella zeae*) is a globally distributed causal agent of Fusarium head blight (FHB) of cereal crops worldwide, especially of wheat (Goswami & Kistler, 2004; Leslie & Summerell, 2006). In addition to the yield losses caused by the infection of cereal spikelets, *F. graminearum* can also produce harmful mycotoxins, including deoxynivalenol (DON) and zearalenone (ZEA), which are extremely toxic to humans and livestock (Audenaert et al., 2014; Desjardins, 1996; Zhang et al., 2016). In the disease cycle of FHB, ascospores (sexual spores) and conidia (asexual spores) play a critical role in primary and secondary infection, respectively (Guenther & Trail, 2005; Trail, 2007). Under favourable environmental conditions, *F. graminearum* spreads rapidly and causes severe grain yield losses. Thus, perithecia formation, ascospore production, and ascospore discharge play crucial roles in the infection cycle of *F. graminearum*. Several genes are involved in the process of sexual reproduction, including conserved signal transduction pathways, protein kinases, transcription factors, and other genes with diverse functions (Geng et al., 2014; Hou et al., 2002; Hu et al., 2014; Son et al., 2011, 2013; Wang et al., 2011; Yun et al., 2015). In most cases, the disruption of these genes causes sexual development to be stopped or delayed at certain specific stages. For instance, *mgv1* and *Gpmk1* deletion mutants are female sterile and fail to reproduce perithecia, whereas *GEA1* and *MID1* are known to

be important for ascospore release in *F. graminearum* (Cavinder et al., 2011; Hou et al., 2002; Jenczmionka et al., 2003; Son et al., 2013). However, lncRNAs involved in the regulation of sexual reproduction have rarely been studied. The identification and functional characterization of lncRNA mutants would provide comprehensive insight into the regulatory mechanisms underlying the sexual development of filamentous fungi.

The major facilitator superfamily (MFS) transport proteins are a large protein family with diverse physiological functions in all living organisms (Yen et al., 2010). The sugar porter (SP) family is the largest branch of the MFS (Pao et al., 1998). In phytopathogenic fungi, MFS proteins have been demonstrated to be involved in the regulation of multidrug resistance and toxin accumulation (Alexander et al., 1999; Choquer et al., 2007; Coleman & Mylonakis, 2009; Kretschmer et al., 2009). In the present study, we discovered an lncRNA, *lncRsp1*, located +99 bp upstream of a putative sugar porter gene, *Fgsp1*. Functional studies showed that the disruption of *Fgsp1* and *lncRsp1* had pleiotropic defects, including on sexual development, virulence, and DON production. Subsequently, silencing and overexpression assays of *lncRsp1* were performed to explore their biological functions. Our results suggest that *lncRsp1* plays an important role in sexual reproduction and regulates the expression of *Fgsp1*.

2 | RESULTS

2.1 | Identification of *lncRsp1* and *Fgsp1*

Based on the sequence analysis of the full-length FGSG_05042 mRNA, the open reading frame (ORF) was determined to encode a protein of 534 amino acids (GenBank accession no. XP_011323525). NCBI domain analysis indicated that the protein contains a sugar transport domain and two MFS conserved domains. Therefore, FGSG_05042 was designated as *Fgsp1* (Figure 1a). Transmembrane domain prediction (<http://www.cbs.dtu.dk/services/TMHMM/>) indicated that *Fgsp1* possesses 12 transmembrane helices (TM) (Figure 1a), suggesting that *Fgsp1* is a member of the 12-TM group of MFS transporters. An lncRNA, referred to as *lncRsp1* here, was detected in the RNA sequencing (RNA-Seq) data. It was located +99 bp upstream of *Fgsp1* and had the same direction as the *Fgsp1* gene. The full-length sequences of *Fgsp1* and *lncRsp1* were determined by performing the rapid amplification of cDNA ends (RACE) and directional sequencing (Figure S1a–c). The results indicated that *Fgsp1* had two transcript isoforms, *Fgsp1-1* and *Fgsp1-2*, which were transcribed from different transcription initiation sites (TISs) and shared the same 3' ends with poly(A) tails (Figure 1c). The *Fgsp1-1* transcript isoform was 1975 nucleotides (nt) in length, overlapping with *lncRsp1-2* by 338 bases, while the *Fgsp1-2* transcript isoform was 2798 nt in length. The TIS of *Fgsp1-2* was located upstream of *Fgsp1-1* and overlapped with the entire sequence of *Fgsp1-1* (Figure 1b). The *Fgsp1-2* TIS was only 72 nt apart from that of *lncRsp1*. The 3' RACE

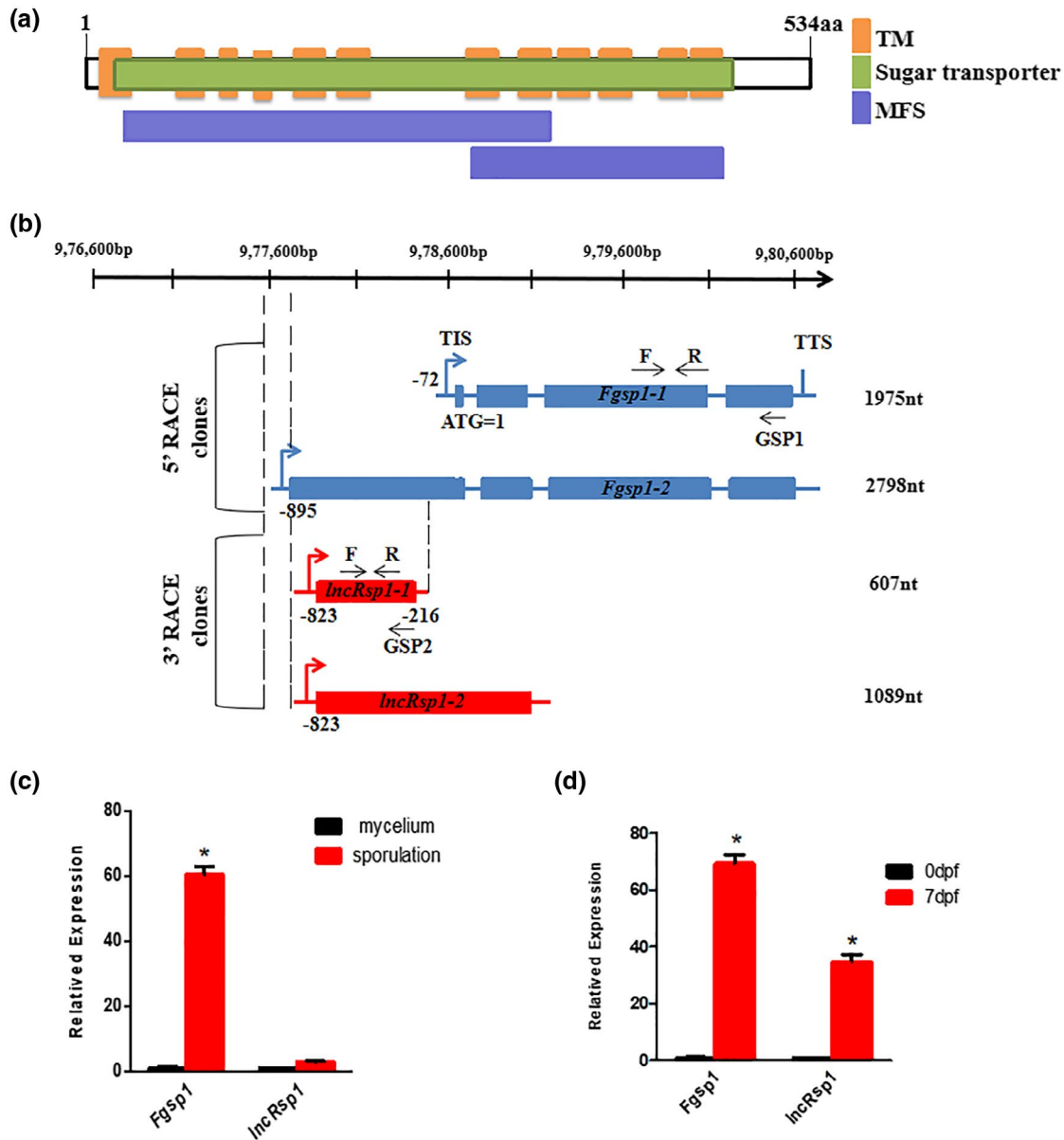


FIGURE 1 The expression pattern of *IncRsp1* and *Fgsp1* during the asexual and sexual stages. (a) The *Fgsp1* amino acid sequence contains a sugar transporter domain (green), two major facilitator superfamily domains (MFS, blue), and 12 transmembrane helices (TM, orange), identified using the SMART protein database (<http://smart.embl-heidelberg.de>) and the NCBI protein database (<https://blast.ncbi.nlm.nih.gov/Blast.cgi>). The transmembrane domain was predicted with the TMHMM Server v. 2.0 (<http://www.cbs.dtu.dk/services/TMHMM/>). (b) Schematic representation of *IncRsp1* and *Fgsp1* transcript regions detected by RACE-PCR analysis. The position of gene-specific primers (GSP) used to assay the expression levels of *IncRsp1* and *Fgsp1* are marked with arrows. nt, nucleotide; F, forward primer; R, reverse primer. (c) Expression levels of *IncRsp1* and *Fgsp1* during asexual stages were measured by reverse transcription quantitative PCR (RT-qPCR). Cultures were collected from YEPD (black) and CMC (red) liquid medium after 3 and 24 h of inoculation as mycelium and sporulation samples, respectively. The expression levels in the mycelium sample were set as the control. The *F. graminearum* β -tubulin gene was used as the internal standard. (d) Expression levels of *IncRsp1* and *Fgsp1* in the sexual stage were detected by RT-qPCR. The mycelium collected from a carrot agar plate at 7 days postinoculation was used as the 0 days postfertilization (dpf) sample (black). Perithecia were collected from a carrot agar plate after 7 days of self-crossing and used as the 7 dpf sample (red). The expression levels in the wild-type strain PH-1 at 0 dpf were set as the control. Results shown represent means \pm SD. Error bars indicate SD calculated from three replicated data points. The asterisks indicate significant differences ($p < 0.01$)

sequences included *IncRsp1-1*, 1089 nt in length, whose transcription termination site (TTS) was adjacent to the second exon of *Fgsp1-1*. *IncRsp1-2*, another 607 nt-lncRNA transcript isoform sharing the same TIS as *IncRsp1-1*, was also located upstream of

Fgsp1-1 (Figure 1b). Although 5' RACE results indicated that *Fgsp1* has two transcript isoforms, *Fgsp1-1* and *Fgsp1-2*, according to our previous RNA-Seq data of the wild-type strain PH-1, few reads could be mapped onto the 5' end of the *Fgsp1-2* transcript isoform

in IGW Sashimi plots at different developmental stages, including sexual development stages (0, 7, and 10 days postfertilization [dpf]), conidial stages (3 [mycelial stage] and 12 h after incubation in CMC liquid medium [sporulation stage]) (Figure S2). This suggested that the *Fgsp1* gene was mainly transcribed as the *Fgsp1-1* transcript isoform at all the different stages. Therefore, we did not consider the effect of *Fgsp1-2* transcript on the other transcript isoforms. Using the reverse transcription quantitative PCR (RT-qPCR) method, the expression levels of the two isoforms of *Fgsp1* and *IncRsp1* were analysed at different developmental stages. The results showed that the expression levels of *Fgsp1* and *IncRsp1* during sporulation were both higher than those during vegetative growth (Figure 1c). During sexual development, both *Fgsp1* and *IncRsp1* were significantly up-regulated at 7 dpf compared with their expression at 0 dpf (Figure 1d).

To determine their biological functions, *Fgsp1* and *IncRsp1* deletion mutants ($\Delta Fgsp1$ and $\Delta IncRsp1$) were generated using a homology recombination strategy. The entire *IncRsp1* transcriptional region (-977,720 to -978,636 of chromosome 3) was deleted in the $\Delta IncRsp1$ mutant, while the $\Delta Fgsp1$ mutant was generated by deletion of the *Fgsp1* transcriptional region (-978,706 to -980,551 of chromosome 3). The mutants were confirmed by PCR amplification and Southern blotting analysis (Figure S3a-c). Meanwhile, the complementary strains of *Fgsp1*, $\Delta Fgsp1$ -C, were constructed to confirm that the defects observed in $\Delta Fgsp1$ were derived from the deletion of *Fgsp1*. In the asexual stage, no obvious differences in hyphal growth, conidiation, or conidial morphology were observed (Figure S4a-c, Table S1). Therefore, neither *Fgsp1* nor *IncRsp1* is essential for asexual reproduction and hyphal growth in *F. graminearum*.

2.2 | *Fgsp1* and *IncRsp1* are involved in sexual reproduction

When we assayed sexual reproduction on carrot agar medium, normal-shaped perithecia and ascospore cirri were produced from all mutants at 7 and 14 dpf, respectively (Figure 2a). However, compared to that of PH-1, the number of discharged ascospores of the $\Delta IncRsp1$ mutant was significantly decreased. Additionally, a more pronounced defect in ascospore discharge was observed in the $\Delta Fgsp1$ mutant (Figure 2b). Subsequently, we examined the ascospores and asci in perithecia sampled at 6, 7, and 10 dpf. At 7 dpf, less than 20% and 40% of asci produced by $\Delta Fgsp1$ and $\Delta IncRsp1$ were type I asci, which contain eight spindle-shaped ascospores, while 65% of asci were type I in PH-1 (Figure 2c,d). In $\Delta Fgsp1$ and $\Delta IncRsp1$, most of the asci were defective, such as abnormal asci with fewer ascospores (type II) or failed to form asci (type III) (Figure 2c,d). Moreover, $\Delta Fgsp1$ and $\Delta IncRsp1$ asci showed significantly reduced glycogen accumulation in comparison with those of the wild type after KI-I₂ staining (Figure 2c). These results indicate that *Fgsp1* and *IncRsp1* are involved in glycogen accumulation, ascus development, and ascospore discharge in *F. graminearum*.

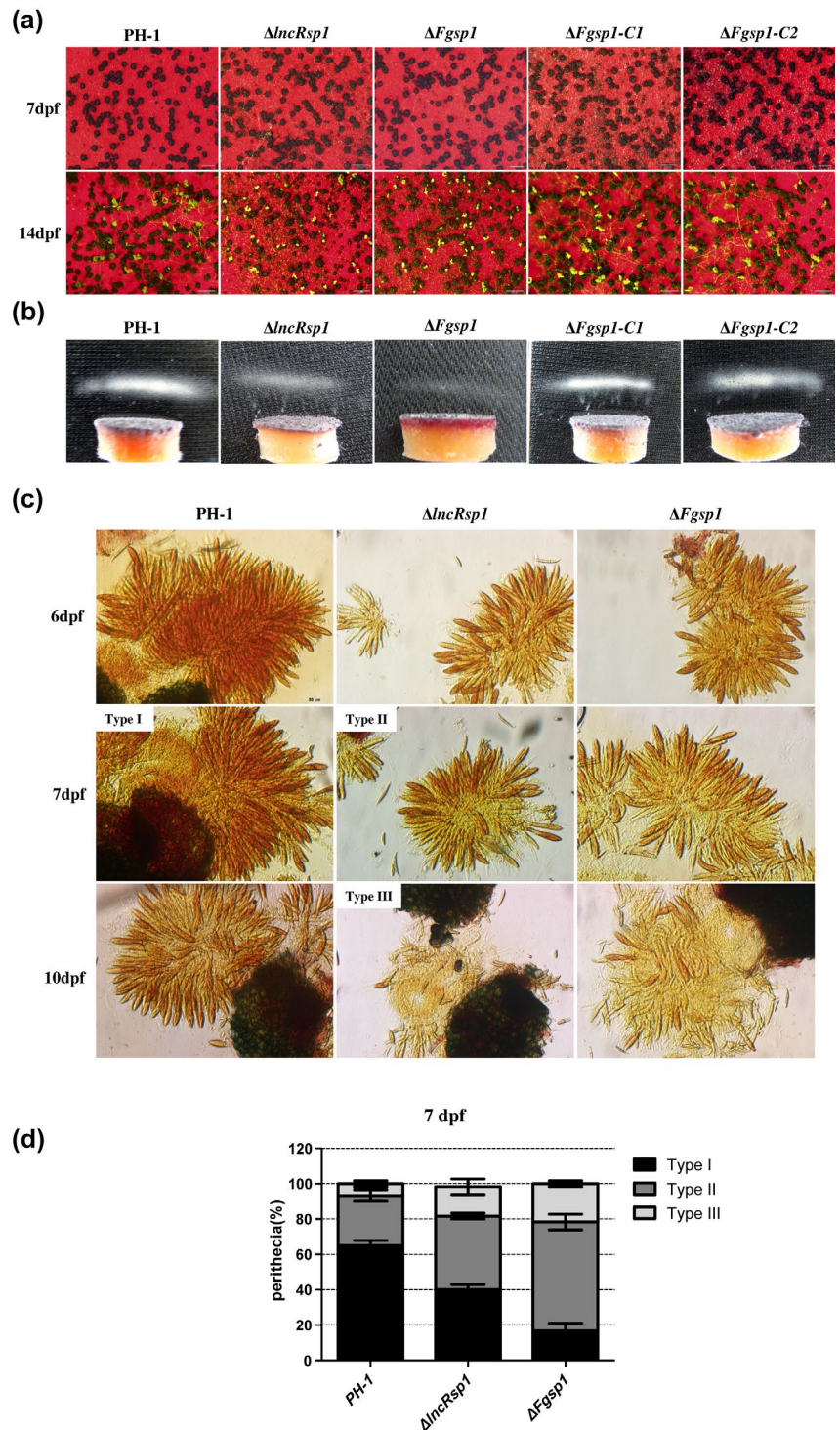
2.3 | *Fgsp1* and *IncRsp1* play crucial roles in the pathogenicity of *F. graminearum*

To investigate the roles of *Fgsp1* and *IncRsp1* in fungal virulence, pathogenicity assays on flowering wheat heads and wheat coleoptiles were conducted. At 14 days postinoculation (dpi), spikes infected with the $\Delta Fgsp1$ and $\Delta IncRsp1$ strains displayed similar symptoms to spikes infected by the wild-type strain (Figure 3a,b). However, when a pathogenicity assay was performed on wheat coleoptiles, the average lengths of the brown lesions caused by the $\Delta Fgsp1$ and $\Delta IncRsp1$ mutants were 0.59 ± 0.26 and 0.54 ± 0.26 cm, respectively, whereas those infected by the wild-type strain showed an average lesion length of 1.03 ± 0.09 cm (Figure 3c,d), indicating a significant reduction in the virulence of the $\Delta Fgsp1$ and $\Delta IncRsp1$ mutants. Thus, *Fgsp1* and *IncRsp1* are required for the virulence of *F. graminearum* to wheat coleoptiles.

2.4 | *Fgsp1* and *IncRsp1* negatively regulate DON production

To detect the production of DON, the mycotoxin produced in infected wheat kernels with scab symptoms at 14 dpi was measured in this study. The DON production (over 1200 ng/kernel) was increased significantly in the $\Delta Fgsp1$ and $\Delta IncRsp1$ mutants compared with the 435 ng/kernel DON produced by the wild-type PH-1 strain (Figure 4a). We further assayed the DON production in rice medium, as described by Seo et al. (1996). Similar to the results of the wheat grain inoculation assay, more DON production was synthesized in rice medium by $\Delta Fgsp1$ and $\Delta IncRsp1$ mutants than by the wild-type strain PH-1 (Figure 4a). These results indicate that *Fgsp1* and *IncRsp1* negatively regulate DON biosynthesis. To further confirm the results, the expression levels of the DON synthesis genes *TRI4*, *TRI5*, *TRI6*, *TRI13*, *TRI101*, and *TRI12* were measured in DON-inducing cultures by a RT-qPCR assay. The results demonstrated that the expression levels of *TRI4*, *TRI5*, *TRI6*, and *TRI13* were significantly up-regulated in the $\Delta Fgsp1$ and $\Delta IncRsp1$ mutants compared to those in the wild type (Figure 4b), which is consistent with the fact that the deletion of *Fgsp1* and *IncRsp1* produced more DON than the wild-type strain in both wheat kernels and rice medium (Figure 4a). Interestingly, the expression levels of *TRI101* and *TRI12* were reduced in the *Fgsp1* mutant (Figure 4c). As these two genes are not located in the same *TRI* cluster, *Fgsp1* probably modulates them through different pathways. Previous research has suggested that hyphal bulbous structures at the toxigenic stage are related to DON production (Jiang et al., 2016). After being incubated in trichothecene biosynthesis induction (TBI) cultures for 5 days, abundant bulbous hyphal structures were observed in PH-1 and the $\Delta IncRsp1$ mutant. However, bulbous structures were rarely observed in the $\Delta Fgsp1$ mutant under the same conditions (Figure 4d). Together, these results showed that *Fgsp1* and *IncRsp1* function as negative regulators in DON biosynthesis by suppressing the expression of four genes relevant to DON synthesis, *TRI4*,

FIGURE 2 Defects of the $\Delta IncRsp1$ and $\Delta Fgsp1$ mutants in sexual reproduction. (a) Morphology of perithecia and cirri of the wild-type PH-1, $\Delta IncRsp1$, and $\Delta Fgsp1$ strains. Perithecia (upper panel) and perithecia with cirri (lower panel) were observed on carrot agar medium. PH-1 strain was used as the control. Photographs were taken at 7 and 14 days postfertilization (dpf) on carrot agar. Bar = 500 μ m. (b) Ascospore discharge was examined using 7-day-old perithecia. Photographs were taken after being released for 18 h. The white cloud is the accumulation of discharged ascospores. (c) Asci morphology and glycogen accumulation from cracked perithecia. The samples were stained with KI-I₂ solution. Bar = 20 μ m. (d) Morphology and statistical analysis of asci rosettes of 7-day-old perithecia. The morphology of type I asci rosettes was selected from the wild-type strain PH-1; type II and type III were selected from $\Delta Fgsp1$. The statistical analysis for each type of ascus morphology was conducted at 7 dpf. A total of 50 asci rosettes were counted and classified in each strain under light microscopy. Line bars indicate standard errors from three repeated experiments



TRI5, *TRI6*, and *TRI13*. Furthermore, *Fgsp1* is also required for DON production-related cellular differentiation.

2.5 | *IncRsp1* positively regulates *Fgsp1* transcript levels

The above results indicate that the expression patterns of *Fgsp1* and *IncRsp1* are similar. Their deletion caused similar defects in

ascospore discharge, virulence, and DON biosynthesis. Previous studies have shown that lncRNAs could affect the expression of their neighbouring genes (Mercer et al., 2009; Rinn & Chang, 2012). To investigate the regulatory relationship between *IncRsp1* and *Fgsp1*, the *Fgsp1* and *IncRsp1* transcript level in the wild type, the $\Delta IncRsp1$ mutant, and the $\Delta Fgsp1$ mutant were measured during sexual stages (cultures grown on carrot agar at 0 and 7 dpf). The *Fgsp1* expression level in the wild-type strain was 105 times higher at 7 dpf than that at 0 dpf, and only six times higher in the $\Delta IncRsp1$ mutant.

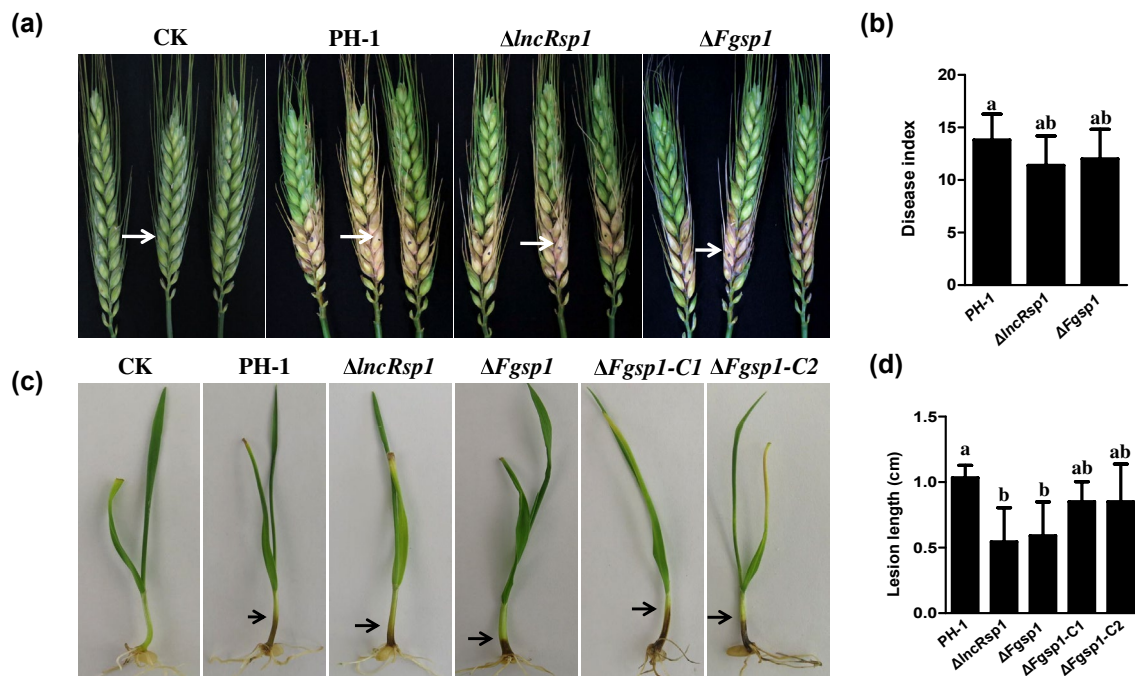


FIGURE 3 Roles of the *IncRsp1* and *Fgsp1* in fungal pathogenicity. (a) Pathogenicity assays on wheat spikelets (marked with black dots) with a conidial suspension of the wild-type PH-1, $\Delta IncRsp1$, $\Delta Fgsp1$ mutants, and $\Delta Fgsp1$ -C1/C2 strains. The photographs were taken 14 days after inoculation. The white arrows indicate the inoculation sites on wheat head. (b) The disease index calculated 14 days after inoculation. (c) Wheat coleoptiles infected with each strain were observed and photographed 7 days after inoculation. The black arrows indicate the lesion. (d) The length of the brown lesions on wheat coleoptiles. Mean and standard deviation were calculated from three repeated experiments. Means of the column with different letters represent a statistically significant difference at $p = 0.05$

Thus, the deletion of *IncRsp1* significantly decreased the expression level of *Fgsp1* at 7 dpf. Similarly, the expression level of *IncRsp1* was also significantly down-regulated by the deletion of *Fgsp1* at 7 dpf (Figure 5a). However, the physical location of *IncRsp1* raised the concern that the *IncRsp1* transcript could be part of the *Fgsp1* transcript and the deletion of *IncRsp1* could cause the disruption of *Fgsp1* itself. To address this concern, *IncRsp1* silencing and overexpression vectors were randomly integrated into the wild-type strain to generate *IncRsp1*-silenced (Si) and -overexpressing (OE) mutant strains, respectively (Figure S5a–d). The expression levels of both *IncRsp1* and *Fgsp1* were significantly up-regulated in the *IncRsp1*-overexpressing strains *IncRsp1*OE-1 and *IncRsp1*OE-3 (Figure 5b). In contrast, the expression levels of both *IncRsp1* and *Fgsp1* in the *IncRsp1*-silenced mutants *IncRsp1*Si-1, *IncRsp1*Si-2, and *IncRsp1*Si-5, were significantly down-regulated compared with the wild-type strain PH-1 (Figure 5c). These results demonstrate that *IncRsp1* is a positive regulator of the *Fgsp1* gene.

To further analyse the function of *IncRsp1* in sexual reproduction, the perithecia and discharged ascospores of *IncRsp1*-silenced and -overexpressing strains were investigated. During sexual differentiation, normal perithecia development and perithecia with cirri were observed at 7 or 14 dpf, respectively (Figure 5d). However, compared with the wild type, the number of discharged ascospores was significantly decreased in *IncRsp1*-silenced strains (Figure 5e,f). In contrast, strains with *IncRsp1* overexpression exhibited a significantly increased ascospore discharge under the same conditions

(Figure 5e,f). These results indicate that *IncRsp1* could enhance ascospore discharge by promoting the expression of *Fgsp1*.

Finally, to confirm that *IncRsp1* indeed plays a direct role in sexual reproduction, the complementary strains of $\Delta IncRsp1$, $\Delta IncRsp1$ -LC (*IncRsp1*-LC-1 and *IncRsp1*-LC-2), were constructed in situ (Figure S6a). The two complementary strains, *IncRsp1*-LC-1 and *IncRsp1*-LC-2, had a similar sexual reproduction ability to that of the wild-type strain (Figure S6b–d). These results further indicate that *IncRsp1* can affect ascospore discharge via regulating the expression of *Fgsp1*.

3 | DISCUSSION

lncRNAs play crucial regulatory roles in many biological processes in several eukaryotes (Quinn & Chang, 2016; Rinn & Chang, 2012; Sun et al., 2018; Till, Mach, et al., 2018). In filamentous fungi, studies of lncRNAs have been reported in *N. crassa*, *F. graminearum*, *U. maydis*, and *T. reesei* (Arthanari et al., 2014; Cemel et al., 2017; Donaldson et al., 2017; Kim et al., 2018). However, to date the biological functions and molecular basis of lncRNA-mediated gene regulation have rarely been studied. Transcriptomes studies have shown a surprising complexity of lncRNAs that are often overlapping with, or interspersed within, multiple coding and noncoding transcripts (Carninci et al., 2005; Ding et al., 2012; Kapranov, 2005). In this study, we discovered and functionally characterized the *IncRsp1* located immediately upstream of *Fgsp1* and transcribed in the same direction as

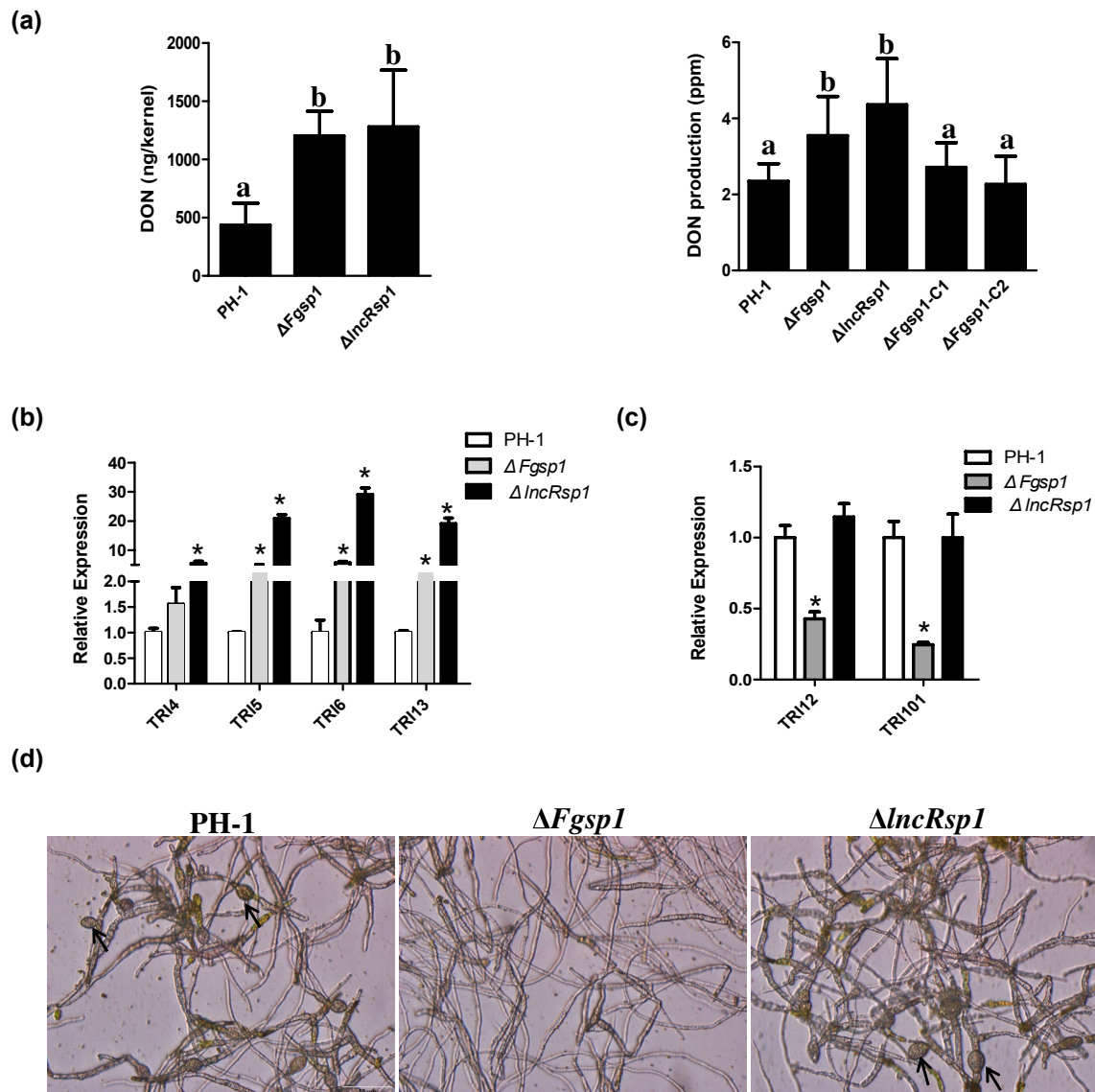


FIGURE 4 *IncRsp1* and *Fgsp1* regulate deoxynivalenol (DON) production and *TRI* gene expression. (a) DON production in 14-day-old infected wheat kernels (left) and 21-day-old rice grain cultures (right) was measured. Data with three replicates were analysed using the protected Fisher's least significant difference (LSD) test. Different letters on the bars indicate statistically significant differences ($p = 0.05$). (b) Relative expression levels of *TRI4*, *TRI5*, *TRI6*, and *TRI13* in the wild-type strain PH-1, $\Delta IncRsp1$, and $\Delta Fgsp1$ were measured by reverse transcription quantitative PCR (RT-qPCR). (c) Relative expression levels of *TRI12* and *TRI101* genes in PH-1, $\Delta IncRsp1$, and $\Delta Fgsp1$ mutants. The expression level in PH-1 was set as 1. Error bars indicate the standard deviation from three biological replicates. The asterisks indicate significant differences ($p < 0.01$). (d) Five-day-old tricothecene biosynthesis induction cultures of the wild-type PH-1 and the $\Delta IncRsp1$ and $\Delta Fgsp1$ mutants were examined to observe bulbous structures (labelled with arrows). Bar = 20 μm

Fgsp1. RACE was performed to determine the transcription start and end sites of *IncRsp1* and *Fgsp1*. Transcriptional analysis revealed two transcripts of *IncRsp1* (*IncRsp1-1* and *IncRsp1-2*) that were transcribed from the same strand and overlapped with each other (Figure 1b). They were defined as lncRNAs because none of them was predicted to encode a protein. The *Fgsp1* gene exhibited two different transcripts of varying lengths (*Fgsp1-1* and *Fgsp1-2*), of which *Fgsp1-2* transcription initiated 72 nt upstream of the *IncRsp1* TIS (Figure 1b). According to our RNA-Seq data of the wild-type strain PH-1, the expression of *Fgsp1-2* was almost undetectable at all stages (Figure S2). Therefore, we thought the main transcript of the gene *Fgsp1* was

Fgsp1-1 isoform. The expression level of *IncRsp1* and *Fgsp1* was up-regulated during sexual reproduction, implying that they were involved in sexual development processes (Figure 1d). Indeed, the number of discharged ascospores of $\Delta IncRsp1$ and $\Delta Fgsp1$ mutants was less than that of the wild-type strain (Figure 2b). In addition, *IncRsp1* and *Fgsp1* were also found to be involved in regulating the virulence and DON production of *F. graminearum*.

The deletion of *IncRsp1* also disrupted the expression of *Fgsp1-2*. However, because the expression level of *Fgsp1-2* isoform was almost undetectable at sexual and asexual stages, we did not consider the effect of *IncRsp1* deletion on the expression of *Fgsp1*. In the *IncRsp1*

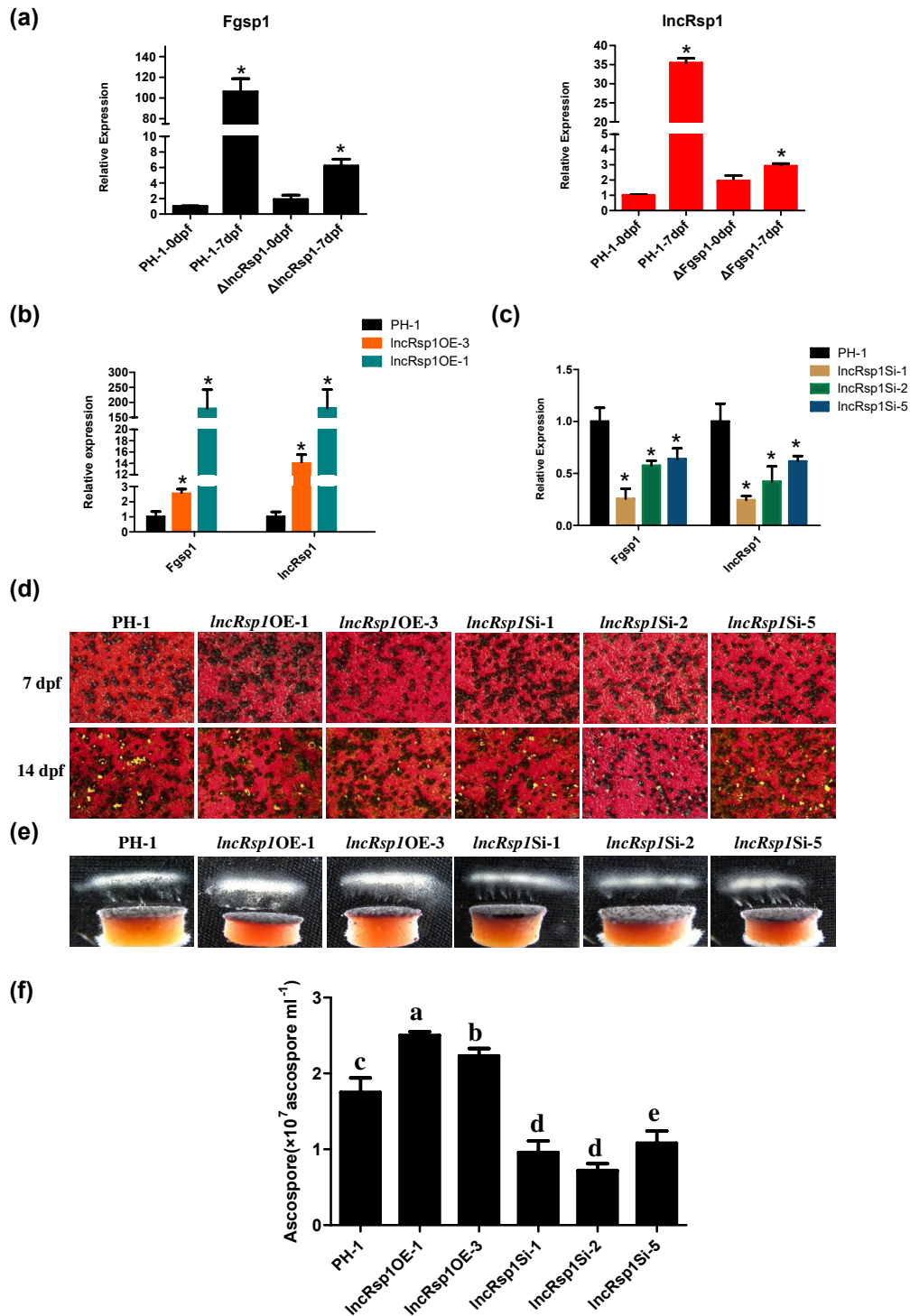


FIGURE 5 *IncRsp1* positively regulates the expression of *Fgsp1*. (a) Relative expression levels of *IncRsp1* and *Fgsp1* in different strains were measured by reverse transcription quantitative PCR (RT-qPCR) during the sexual stage. The expression of *Fgsp1* in the wild-type strain PH-1 at 0 days postfertilization (dpf) was set as the control. (b) Relative expression levels of *Fgsp1* and *IncRsp1* in PH-1 and *IncRsp1*-overexpressing (OE) strains were measured by RT-qPCR. (c) Relative expression levels of *Fgsp1* and *IncRsp1* in PH-1 and *IncRsp1*-silenced (Si) strains. In all panels, the results shown represent means \pm SD. Bars indicate the SD of three replicates. The expression of *Fgsp1* in the wild-type strain PH-1 at 7 dpf was set as the control. (d) Perithecia and cirrhi of *IncRsp1Si* and *IncRsp1OE* transformants. Bar = 500 μ m. (e) The ascospores discharged from 7-day-old mature perithecia. Pictures were taken 18 h after the experiment was initiated. (f) The number of the discharged ascospores. Error bars represent the standard deviations of three repeated experiments. Different letters on the bars indicate statistically significant differences ($p = 0.01$)

deletion mutant only the transcriptional region of *IncRsp1* excluding the transcription start site of *Fgsp1-1* was deleted. To further clarify whether deletion of *IncRsp1* disrupted the promoter of *Fgsp1-1*, the complementary mutant strains of *IncRsp1* were constructed in situ, as shown in Figure S6a. The complementary mutants *IncRsp1*-LC1/LC2 fully restored the ascospore discharge defects of Δ *IncRsp1* mutants (Figure S6c), indicating that deletion of *IncRsp1* did not disrupt the function of the promoter of *Fgsp1-1*. Given the modest effect on the *Fgsp1-1* transcript level by the disruption of *IncRsp1*, we also constructed the *IncRsp1*-silenced strains *IncRsp1Si* and overexpression strains *IncRsp1OE* by random integration of the vectors into the wild-type strain (Figure S5a,c). The expression of *Fgsp1* was significantly reduced in the *IncRsp1Si* strains, while it was increased dramatically in the *IncRsp1OE* strains at the sexual stage (Figure 5b,c). In terms of sexual reproduction, the number of discharged ascospores in *IncRsp1Si* strains was slightly lower than that of the wild-type strain PH-1 (Figure 5d,f). Consistent with expectations, *IncRsp1OE* strains enhanced the ability of the ascospore discharge (Figure 5e,f). Although silencing of *IncRsp1* might also result in the silence of *Fgsp1-2*, considering that the expression level of *Fgsp1-2* isoform was very low at both sexual and sporulation stages, we did not analyse the effect of the *IncRsp1* silencing on *Fgsp1-2* expression. At the same time, random integration of the *IncRsp1* overexpression vector also avoids affecting the promoter of *Fgsp1* due to the close distance between *IncRsp1* and *Fgsp1*. Therefore, the above results suggest that *IncRsp1* can affect the sexual development of *F. graminearum* by regulating the expression of *Fgsp1*. Lots of studies have confirmed that lncRNAs can regulate the expression of their neighbouring coding genes via *trans* or *cis* regulation (Engreitz et al., 2016; Yin et al., 2015). In our study, considering exogenous *IncRsp1* was randomly integrated into the *F. graminearum* genome, we concluded that *IncRsp1* is a crucial *trans*-acting regulator of *Fgsp1* transcription.

In *F. graminearum*, DON was widely considered as an important virulence effector (Chen et al., 2019). In this study, the deletion of *Fgsp1* and *IncRsp1* caused a significant increase in DON production, which indicated that *Fgsp1* and *IncRsp1* negatively regulate DON production (Figure 4a). Previous work has found that the expression level of *TRI* genes was associated with DON production (Chen et al., 2019). In this study, the expression level of four *TRI* genes (*TRI4*, *TRI5*, *TRI6*, and *TRI13*) was significantly up-regulated in Δ *Fgsp1* and Δ *IncRsp1* mutants, which was consistent with the results of the DON production assay. However, *TRI12* and *TRI101*, known as self-defence genes for mycotoxin in *Fusarium* spp. (Alexander et al., 1999; Garvey et al., 2008; Menke et al., 2012), reduced expression levels in Δ *Fgsp1* mutant (Figure 4c). This result indicated that *Fgsp1* might play divergent roles in the DON synthesis pathway. Furthermore, the deletion of *Fgsp1* affected the normal hyphal bulbous structure formation in DON-inducing medium, but no obvious difference was observed between the Δ *IncRsp1* mutant and wild-type strains (Figure 4d), suggesting that the functional relationship between *Fgsp1* and *IncRsp1* varies in regulating DON biosynthesis. It is worth noting that although DON biosynthesis was increased in the *Fgsp1* deletion mutant, it rarely formed the hyphal bulbous structures associated with

DON production. Previous research has found that, unlike *Fgsp1*, the *tri6 pde2* mutant fails to produce DON but has increased bulbous structures (Jiang et al., 2016). As the hyphal bulbous structures formed before *TRI* gene transcription are closely related to DON production in *F. graminearum* (Jonkers et al., 2012), the absence of bulbous structures caused by the deletion of *Fgsp1* seemed to be independent of *TRI* genes. However, further studies are needed to identify the underlying regulatory mechanisms.

Sexual reproduction is an important developmental process in the disease cycle of FHB. Ascospores, which are forcibly discharged into air from perithecia, play a crucial role in fungal survival and disease propagation (Guenther & Trail, 2005; Trail et al., 2002). Our data showed that the Δ *IncRsp1* and Δ *Fgsp1* mutants produced more abnormal asci and significantly reduced ascospore discharge and glycogen accumulation (Figure 2b,c), indicating that *IncRsp1* and *Fgsp1* are essential for sexual reproduction in *F. graminearum*. Previous work has demonstrated that the turgor pressure within the extended asci is necessary for the forcible discharge of ascospores (Trail, 2007). The build-up of ion fluxes, especially in K^+ , Na^+ , Cl^- , and Ca^{2+} ion channels and glycogen accumulation, is tightly related to the generation of turgor pressure (Min et al., 2010; Trail et al., 2002, 2005). Thus, it is likely that the reduced number of discharged ascospores observed in *IncRsp1* and *Fgsp1* deletion mutants is due to the developmental defects of asci and the decrease in glycogen accumulation.

In conclusion, our results indicate that *IncRsp1* and *Fgsp1* are important for the sexual reproduction, DON production, and pathogenesis of *F. graminearum*, while *IncRsp1* plays a crucial regulatory role in the expression of *Fgsp1*. Although the underlying mechanism remains undefined, our findings not only help to further understand the molecular mechanism of the sexual reproduction of *F. graminearum* but also promote the understanding of the role of lncRNA in plant pathogenic fungi.

4 | EXPERIMENTAL PROCEDURES

4.1 | Fungal strains and culture conditions

The *F. graminearum* strain PH-1 (NRRL 31084) (Trail & Common, 2000) and all mutant strains were cultured on potato dextrose agar (PDA) plates at 25°C in the dark. The colony morphology, growth rate, and conidial germination were measured on PDA, minimum medium (MM), and complete medium (CM) plates incubated at 25°C for 3 days. For conidiation tests, the conidia were induced in carboxymethylcellulose (CMC) liquid culture medium (1 g NH_4NO_3 , 1 g KH_2PO_3 , 0.5 g $MgSO_4 \cdot 7H_2O$, 1 g yeast extract, 15 g CMC, and 1 L water). The 5-mm mycelial agar blocks were incubated in 4 ml of CMC medium at 25°C for 5 days in a rotary shaker (200 rpm). Conidia were collected in distilled water by filtration. The conidial morphology was observed under a fluorescence microscope. The number of conidia produced by each strain was counted using a haemocytometer (Cappellini & Peterson, 1965). Conidial germination rates were assayed as described previously (Zhou et al., 2010).

The conidial suspension (10^6 conidia/ml) was harvested and then inoculated into yeast extract peptone dextrose (YEPD) (0.3% yeast extract, 1% peptone, 2% dextrose) liquid medium at 25°C in a shaker (200 rpm). The conidial germination was observed after 6 h of incubation. The sexual development, including perithecium formation, cirrus production, ascus development, and ascospore discharge, was performed as previously described (Wang et al., 2021; Zeng et al., 2018). All strains were grown on carrot agar plates under near-ultraviolet light at 25°C for 7 days. Perithecium formation and cirrus production were observed 1–2 weeks after fertilization. Perithecia and cirri samples were observed with an Olympus IX71 microscope and Olympus cellsens standard camera software. The glycogen staining of asci was performed as described previously (da Rocha Campos & Costa, 2010). Ascospore discharge assays were also performed as previously described (Trail et al., 2002). Carrot agar (10 mm in diameter) covered with mature perithecia cultures was cut in half and placed inverted on a coverslip in a humidity box for 18 h, and the images were captured using a camera. The number of discharged ascospores was counted as follows. Ascospores were collected by placing the carrot agar upside down for 10 h and allowing the mature perithecia to discharge ascospores on Petri dish covers. Ascospores were completely harvested from the Petri dish lids in distilled water and the number of ascospores was counted under a microscope.

4.2 | Plant infection, DON production assays, and expression levels of *TRI* genes

Pathogenicity assays on wheat spikes and coleoptiles were conducted as described previously (Hou et al., 2002; Seong et al., 2005; Wu et al., 2005). A 2- μ l aliquot of conidial suspension (5×10^5 conidia/ml in sterile distilled water) of each strain was used to inoculate each of 20 coleoptiles of 3-day-old wheat seedlings with three replicates in a growth chamber. Two microlitres of 0.01% Tween 20 solution was inoculated as a control. The lesion size of each strain was counted and analysed at 7 dpi. Virulence assays on flowering wheat heads were performed as previously described (Hou et al., 2002). To this end, 10 μ l of 10^5 conidia/ml suspension, collected from 5-day-old CMC cultures, was inoculated onto the fifth flowering spikelet of wheat variety Zhengmai 9023. The experiment was carried out with three independent replicates. The disease index for each strain was calculated as described by Luo et al. (2014). The number of symptomatic spikelets was counted and images were captured 14 days after inoculation.

To measure the DON production, the infected wheat kernels with typical FHB symptoms were harvested for DON assays as previously described (Tian et al., 2020). DON production in rice cultures was assayed as described (Bluhm et al., 2007; Seo et al., 1996). To determine the expression levels of *TRI* genes (*TRI4*, *TRI5*, *TRI6*, *TRI12*, *TRI13*, *TRI101*), conidia of each strain were inoculated into TBI medium (Gardiner et al., 2009) and cultured for 3 days at 25°C in a shaker (200 rpm). Mycelia of each sample were harvested and total RNA was extracted. The expression levels of *TRI* genes were

determined by RT-qPCR assays with the primers listed in Table S2. The experiment was repeated three times independently.

4.3 | RT-qPCR detection of *IncRsp1* and *Fgsp1*

Total RNA was isolated using the TRIzol reagent (Invitrogen) and the first-strand cDNA synthesis was carried out by the EasyScript One-step gDNA removal and cDNA Synthesis SuperMix (Transgen Biotech), according to the manufacturer's instructions. qPCR was performed on a CFX96 Real-Time PCR Detection System (Bio-Rad) with the iTaq Universal SYBR Green Supermix (Bio-Rad). In the conidia stage, the total RNA samples of the wild type were extracted at 3 h (mycelial stage) and 24 h (sporulation stage) after incubation in CMC liquid medium. During sexual development, the RNA samples were isolated from 7-day-old carrot agar plate hyphae (0 dpf) and 7-day-old perithecia (7 dpf). The *F. graminearum* β -tubulin gene (FGSG_09530) was used as an endogenous reference and gene-specific primers (GSP) were used to detect mRNA and lncRNA, respectively. The relative expression of each gene was calculated with the $2^{-\Delta\Delta Ct}$ method. RT-qPCR data from three biological replicates for each sample were calculated from the mean \pm SD (Livak & Schmittgen, 2001). All the primer sequences are provided in Table S2.

4.4 | RACE-PCR assays

Using 5'- and 3'-RACE experiments analysing the transcriptional start and end sites of *IncRsp1* and *Fgsp1*, the sequence was determined by RACE-PCR using the SMARTer RACE 5'/3' Kit (Clontech). All the RACE primers are provided in Table S2.

4.5 | Construction of the *Fgsp1* and *IncRsp1* deletion mutants and complementation strains

The strategy for *Fgsp1* and *IncRsp1* deletion is illustrated in Figure S3. We used a split-marker system, replacing the two genes with the hygromycin resistance gene (*hph*) and the geneticin resistance cassette (*gen*), respectively (Catlett et al., 2003; Zeng et al., 2018). Transformants were selected using the PDA plates amended with 225 μ g/ml hygromycin B (Sigma-Aldrich) or 300 μ g/ml geneticin (Sigma-Aldrich). The *Fgsp1* and *IncRsp1* deletion mutants were identified by PCR with the relevant primers listed in Table S2 and further confirmed by Southern blot analysis (Leslie & Summerell, 2006).

For Southern blotting, the genomic DNA of PH-1 and mutants was extracted according to the *Fusarium* laboratory manual and then digested with *Xho*I. Southern blotting was performed using the Amersham AlkPhos Direct Labeling and Detection System (GE Healthcare). The probe primers are listed in Table S2 and the probes were labelled with alkaline phosphatase.

For complementation assays, the *Fgsp1* fragment including its promoter region was amplified with primers *Fgsp1*-CF and *Fgsp1*-CR,

and cloned into the same sites of vector neoP3300 to generate the *Fgsp1* complementary vector (Yang et al., 2016). The vector was transformed into the $\Delta Fgsp1$ mutant by random integration, and the resultant strain was designated as $\Delta Fgsp1$ -C. The complementation strategy of *IncRsp1* is illustrated in Figure S6a. The complementary fragments were constructed by fusing the hygromycin resistance gene and full-length *IncRsp1* by double-joint PCR according to a previously described method (Liu et al., 2020). The fusion constructs were transformed into the $\Delta IncRsp1$ mutant, as described above, except that hygromycin was used as screening agent.

4.6 | Generation of the *IncRsp1Si* and *IncRsp1OE* transformants

The *IncRsp1* RNAi vector construction was carried out as described previously (Yu et al., 2012; Zhu et al., 2013). To amplify the sense and antisense fragments of *IncRsp1*, the primers *IncRsp1Si1F/IncRsp1Si1R* (sense fragment) and *IncRsp1Si2F/IncRsp1Si2R* (antisense fragment) were used. The amplified *IncRsp1* sense and antisense fragments were subsequently ligated into pCIT to generate a new vector. The newly constructed vector was then digested with *XhoI* and *SacI* to obtain the repeat fragment, then subsequently ligated with the pCH vector to construct pSi *IncRsp1* silencing vector, which was then transformed into the wild-type strain PH-1 by random integration, as previously reported (Yu et al., 2012). *IncRsp1*-overexpressing strains were generated using the pCETH2 vector. The PCR amplification and ligation of the full-length *IncRsp1* into the pCETH2 vector was carried out. Then, the vector was transformed into the wild-type strain PH-1 using the *Agrobacterium*-mediated transformation system by random integration, as described by Yu et al. (2012). The *IncRsp1* transcript level in silenced strains and overexpressing strains was determined by RT-qPCR.

ACKNOWLEDGEMENTS

This work was supported by National Natural Science Foundation of China (31301614 and 31901840).

CONFLICT OF INTEREST

The authors declare that they have no conflict of interest.

DATA AVAILABILITY STATEMENT

The data that support the findings of this study are available from the corresponding author upon reasonable request.

ORCID

Jiasen Cheng  <https://orcid.org/0000-0003-0040-2360>

Yang Lin  <https://orcid.org/0000-0003-3942-7063>

REFERENCES

- Alexander, N.J., McCormick, S.P. & Hohn, T.M. (1999) TRI12, a trichothecene efflux pump from *Fusarium sporotrichioides*: gene isolation and expression in yeast. *Molecular and General Genetics*, 261, 977–984.

- Arthanari, Y., Heintzen, C., Griffiths-Jones, S. & Crosthwaite, S.K. (2014) Natural antisense transcripts and long non-coding RNA in *Neurospora crassa*. *PLoS One*, 9, e91353.
- Audenaert, K., Vanheule, A., Hofte, M. & Haesaert, G. (2014) Deoxynivalenol: a major player in the multifaceted response of *Fusarium* to its environment. *Toxins*, 6, 1–19.
- Belden, W.J., Lewis, Z.A., Selker, E.U., Loros, J.J. & Dunlap, J.C. (2011) CHD1 remodels chromatin and influences transient DNA methylation at the clock gene frequency. *PLoS Genetics*, 7, e1002166.
- Bluhm, B.H., Zhao, X., Flaherty, J.E., Xu, J.R. & Dunkle, L.D. (2007) RAS2 regulates growth and pathogenesis in *Fusarium graminearum*. *Molecular Plant-Microbe Interactions*, 20, 627–636.
- Cappellini, R.A. & Peterson, J.L. (1965) Macroconidium formation in submerged cultures by a non-sporulating strain of *Gibberella zeae*. *Mycologia*, 57, 962–966.
- Carninci, P., Kasukawa, T., Katayama, S., Gough, J., Frith, M.C., Maeda, N. et al. (2005) The transcriptional landscape of the mammalian genome. *Science*, 309, 1559–1563.
- Catlett, N.L., Lee, B.-N., Yoder, O.C. & Turgeon, B.G. (2003) Split-marker recombination for efficient targeted deletion of fungal genes. *Fungal Genetics Reports*, 50, 9–11.
- Cavinder, B., Hamam, A., Lew, R.R. & Trail, F. (2011) Mid1, a mechanosensitive calcium ion channel, affects growth, development, and ascospore discharge in the filamentous fungus *Gibberella zeae*. *Eukaryotic Cell*, 10, 832–841.
- Cemel, I.A., Ha, N., Schermann, G., Yonekawa, S. & Brunner, M. (2017) The coding and noncoding transcriptome of *Neurospora crassa*. *BMC Genomics*, 18, 978.
- Chen, Y., Kistler, H.C. & Ma, Z. (2019) *Fusarium graminearum* trichothecene mycotoxins: biosynthesis, regulation, and management. *Annual Review of Phytopathology*, 57, 15–39.
- Choquer, M., Lee, M.H., Bau, H.J. & Chung, K.R. (2007) Deletion of a MFS transporter-like gene in *Cercospora nicotianae* reduces cercosporin toxin accumulation and fungal virulence. *FEBS Letters*, 581, 489–494.
- Coleman, J.J. & Mylonakis, E. (2009) Efflux in fungi: la piece de resistance. *PLoS Pathogens*, 5, e1000486.
- Desjardins, A.E. (1996) Reduced virulence of trichothecene-nonproducing mutants of *Gibberella zeae* in wheat field tests. *Molecular Plant-Microbe Interactions*, 9, 775–781.
- Ding, J., Lu, Q., Ouyang, Y., Mao, H., Zhang, P., Yao, J. et al. (2012) A long noncoding RNA regulates photoperiod-sensitive male sterility, an essential component of hybrid rice. *Proceedings of the National Academy of Sciences of the United States of America*, 109, 2654–2659.
- Donaldson, M.E., Ostrowski, L.A., Goulet, K.M. & Saville, B.J. (2017) Transcriptome analysis of smut fungi reveals widespread intergenic transcription and conserved antisense transcript expression. *BMC Genomics*, 18, 340.
- Donaldson, M.E. & Saville, B.J. (2013) *Ustilago maydis* natural antisense transcript expression alters mRNA stability and pathogenesis. *Molecular Microbiology*, 89, 29–51.
- Engreitz, J.M., Haines, J.E., Perez, E.M., Munson, G., Chen, J., Kane, M. et al. (2016) Local regulation of gene expression by lncRNA promoters, transcription and splicing. *Nature*, 539, 452–455.
- Gardiner, D.M., Kazan, K. & Manners, J.M. (2009) Nutrient profiling reveals potent inducers of trichothecene biosynthesis in *Fusarium graminearum*. *Fungal Genetics and Biology*, 46, 604–613.
- Garvey, G.S., McCormick, S.P. & Raymont, I. (2008) Structural and functional characterization of the TRI101 trichothecene 3-O-acetyltransferase from *Fusarium sporotrichioides* and *Fusarium graminearum*: kinetic insights to combating *Fusarium* head blight. *Journal of Biological Chemistry*, 283, 1660–1669.
- Geng, Z., Zhu, W., Su, H., Zhao, Y., Zhang, K.Q. & Yang, J. (2014) Recent advances in genes involved in secondary metabolite synthesis, hyphal development, energy metabolism and pathogenicity in

- Fusarium graminearum* (teleomorph *Gibberella zeae*). *Biotechnology Advances*, 32, 390–402.
- Goswami, R.S. & Kistler, H.C. (2004) Heading for disaster: *Fusarium graminearum* on cereal crops. *Molecular Plant Pathology*, 5, 515–525.
- Guenther, J.C. & Trail, F. (2005) The development and differentiation of *Gibberella zeae* (anamorph: *Fusarium graminearum*) during colonization of wheat. *Mycologia*, 97, 229–237.
- Heo, J.B. & Sung, S. (2011) Vernalization-mediated epigenetic silencing by a long intronic noncoding RNA. *Science*, 331, 76–79.
- Hou, Z., Xue, C., Peng, Y., Katan, T., Kistler, H.C. & Xu, J.R. (2002) A mitogen-activated protein kinase gene (MGV1) in *Fusarium graminearum* is required for female fertility, heterokaryon formation, and plant infection. *Molecular Plant-Microbe Interactions*, 15, 1119–1127.
- Hu, S., Zhou, X., Gu, X., Cao, S., Wang, C. & Xu, J.R. (2014) The cAMP-PKA pathway regulates growth, sexual and asexual differentiation, and pathogenesis in *Fusarium graminearum*. *Molecular Plant-Microbe Interactions*, 27, 557–566.
- Jenczmionka, N.J., Maier, F.J., Losch, A.P. & Schafer, W. (2003) Mating, conidiation and pathogenicity of *Fusarium graminearum*, the main causal agent of the head-blight disease of wheat, are regulated by the MAP kinase gpmk1. *Current Genetics*, 43, 87–95.
- Jiang, C., Zhang, C., Wu, C., Sun, P., Hou, R., Liu, H. et al. (2016) TRI6 and TRI10 play different roles in the regulation of deoxynivalenol (DON) production by cAMP signalling in *Fusarium graminearum*. *Environmental Microbiology*, 18, 3689–3701.
- Jonkers, W., Dong, Y., Broz, K. & Kistler, H.C. (2012) The Wor1-like protein Fgp1 regulates pathogenicity, toxin synthesis and reproduction in the phytopathogenic fungus *Fusarium graminearum*. *PLoS Pathogens*, 8, e1002724.
- Kapranov, P. (2005) Examples of the complex architecture of the human transcriptome revealed by RACE and high-density tiling arrays. *Genome Research*, 15, 987–997.
- Kim, W., Miguel-Rojas, C., Wang, J., Townsend, J.P. & Trail, F. (2018) Developmental dynamics of long noncoding RNA expression during sexual fruiting body formation in *Fusarium graminearum*. *mBio*, 9, e01292-18.
- Kretschmer, M., Leroch, M., Mosbach, A., Walker, A.-S., Fillinger, S., Mernke, D. et al. (2009) Fungicide-driven evolution and molecular basis of multidrug resistance in field populations of the grey mould fungus *Botrytis cinerea*. *PLoS Pathogens*, 5, e1000696.
- Leslie, J.F. & Summerell, B.A. (2006) *The Fusarium Laboratory Manual*. Ames, IA, USA: Blackwell Publishing.
- Li, N., Joska, T.M., Ruesch, C.E., Coster, S.J. & Belden, W.J. (2015) The frequency natural antisense transcript first promotes, then represses, frequency gene expression via facultative heterochromatin. *Proceedings of the National Academy of Sciences of the United States of America*, 112, 4357–4362.
- Liu, X., Xie, J., Fu, Y., Jiang, D., Chen, T. & Cheng, J. (2020) The subtilisin-like protease Bcser2 affects the sclerotial formation, conidiation and virulence of *Botrytis cinerea*. *International Journal of Molecular Sciences*, 21, 603.
- Livak, K.J. & Schmittgen, T.D. (2001) Analysis of relative gene expression data using real-time quantitative PCR and the $2^{-\Delta\Delta CT}$ method. *Methods*, 25, 402–408.
- Luo, Y., Zhang, H., Qi, L., Zhang, S., Zhou, X., Zhang, Y. et al. (2014) FgKin1 kinase localizes to the septal pore and plays a role in hyphal growth, ascospore germination, pathogenesis, and localization of Tub1 β -tubulins in *Fusarium graminearum*. *New Phytologist*, 204, 943–954.
- Martens, J.A., Laprade, L. & Winston, F. (2004) Intergenic transcription is required to repress the *Saccharomyces cerevisiae* SER3 gene. *Nature*, 429, 571–574.
- Martianov, I., Ramadass, A., Serra Barros, A., Chow, N. & Akoulitchev, A. (2007) Repression of the human dihydrofolate reductase gene by a non-coding interfering transcript. *Nature*, 445, 666–670.
- Menke, J., Dong, Y. & Kistler, H.C. (2012) *Fusarium graminearum* Tri12p influences virulence to wheat and trichothecene accumulation. *Molecular Plant-Microbe Interactions*, 25, 1408–1418.
- Mercer, T.R., Dinger, M.E. & Mattick, J.S. (2009) Long non-coding RNAs: insights into functions. *Nature Reviews Genetics*, 10, 155–159.
- Min, K., Lee, J., Kim, J.C., Kim, S.G., Kim, Y.H., Vogel, S. et al. (2010) A novel gene, ROA, is required for normal morphogenesis and discharge of ascospores in *Gibberella zeae*. *Eukaryotic Cell*, 9, 1495–1503.
- Ostrowski, L.A. & Saville, B.J. (2017) Natural antisense transcripts are linked to the modulation of mitochondrial function and teliospore dormancy in *Ustilago maydis*. *Molecular Microbiology*, 103, 745–763.
- Pao, S.S., Paulsen, I.T. & Saier, M.H. (1998) Major facilitator superfamily. *Microbiology and Molecular Biology Reviews*, 62, 1–34.
- Ponting, C.P., Oliver, P.L. & Reik, W. (2009) Evolution and functions of long noncoding RNAs. *Cell*, 136, 629–641.
- Quan, M., Chen, J. & Zhang, D. (2015) Exploring the secrets of long noncoding RNAs. *International Journal of Molecular Sciences*, 16, 5467–5496.
- Quinn, J.J. & Chang, H.Y. (2016) Unique features of long non-coding RNA biogenesis and function. *Nature Reviews Genetics*, 17, 47–62.
- Rinn, J.L. & Chang, H.Y. (2012) Genome regulation by long noncoding RNAs. *Annual Review of Biochemistry*, 81, 145–166.
- Rinn, J.L., Kertesz, M., Wang, J.K., Squazzo, S.L., Xu, X., Bruggmann, S.A. et al. (2007) Functional demarcation of active and silent chromatin domains in human HOX loci by noncoding RNAs. *Cell*, 129, 1311–1323.
- da Rocha Campos, A.N. & Costa, M.D. (2010) Histochemistry and storage of organic compounds during basidiosporogenesis in the ectomycorrhizal fungus *Pisolithus microcarpus*. *World Journal of Microbiology and Biotechnology*, 26, 1745–1753.
- Seo, J.A., Kim, J.C., Lee, D.H. & Lee, Y.W. (1996) Variation in 8-ketotrichothecenes and zearalenone production by *Fusarium graminearum* isolates from corn and barley in Korea. *Mycopathologia*, 134, 31–37.
- Seong, K., Hou, Z., Tracy, M., Kistler, H.C. & Xu, J.R. (2005) Random insertional mutagenesis identifies genes associated with virulence in the wheat scab fungus *Fusarium graminearum*. *Phytopathology*, 95, 744–750.
- Son, H., Lee, J. & Lee, Y.W. (2013) A novel gene, *GEA1*, is required for ascus cell-wall development in the ascomycete fungus *Fusarium graminearum*. *Microbiology*, 159, 1077–1085.
- Son, H., Seo, Y.-S., Min, K., Park, A.R., Lee, J., Jin, J.-M. et al. (2011) A phenotype-based functional analysis of transcription factors in the cereal head blight fungus, *Fusarium graminearum*. *PLoS Pathogens*, 7, e1002310.
- Sun, X., Zheng, H. & Sui, N. (2018) Regulation mechanism of long non-coding RNA in plant response to stress. *Biochemical and Biophysical Research Communications*, 503, 402–407.
- Swiezewski, S., Liu, F., Magusin, A. & Dean, C. (2009) Cold-induced silencing by long antisense transcripts of an *Arabidopsis* Polycomb target. *Nature*, 462, 799–802.
- Tang, J., Chen, X., Yan, Y., Huang, J., Luo, C., Tom, H. et al. (2021) Comprehensive transcriptome profiling reveals abundant long non-coding RNAs associated with development of the rice false smut fungus, *Ustilaginoidea virens*. *Environmental Microbiology*, 23, 4998–5013.
- Tian, B., Xie, J., Fu, Y., Cheng, J., Li, B.O., Chen, T. et al. (2020) A cosmopolitan fungal pathogen of dicots adopts an endophytic lifestyle on cereal crops and protects them from major fungal diseases. *The ISME Journal*, 14, 3120–3135.
- Till, P., Mach, R.L. & Mach-Aigner, A.R. (2018) A current view on long non-coding RNAs in yeast and filamentous fungi. *Applied Microbiology and Biotechnology*, 102, 7319–7331.
- Till, P., Pucher, M.E., Mach, R.L. & Mach-Aigner, A.R. (2018) A long non-coding RNA promotes cellulase expression in *Trichoderma reesei*. *Biotechnology for Biofuels*, 11, 78.
- Trail, F. (2007) Fungal cannons: explosive spore discharge in the Ascomycota. *FEMS Microbiology Letters*, 276, 12–18.
- Trail, F. & Common, R. (2000) Perithecial development by *Gibberella zeae*: a light microscopy study. *Mycologia*, 92, 130–138.

- Trail, F., Gaffoor, I. & Vogel, S. (2005) Ejection mechanics and trajectory of the ascospores of *Gibberella zeae* (anamorph *Fusarium graminearum*). *Fungal Genetics and Biology*, 42, 528–533.
- Trail, F., Xu, H., Loranger, R. & Gadoury, D. (2002) Physiological and environmental aspects of ascospore discharge in *Gibberella zeae* (anamorph *Fusarium graminearum*). *Mycologia*, 94, 181–189.
- Wang, C., Zhang, S., Hou, R., Zhao, Z., Zheng, Q., Xu, Q. et al. (2011) Functional analysis of the kinome of the wheat scab fungus *Fusarium graminearum*. *PLoS Pathogens*, 7, e1002460.
- Wang, J., Zeng, W., Xie, J., Fu, Y., Jiang, D., Lin, Y. et al. (2021) A novel antisense long noncoding RNA participates in asexual and sexual reproduction by regulating the expression of *GzmetE* in *Fusarium graminearum*. *Environmental Microbiology*, 23, 4939–4955.
- Wu, A.B., Li, H.P., Zhao, C.S. & Liao, Y.C. (2005) Comparative pathogenicity of *Fusarium graminearum* isolates from China revealed by wheat coleoptile and floret inoculations. *Mycopathologia*, 160, 75–83.
- Xue, Z., Ye, Q., Anson, S.R., Yang, J., Xiao, G., Kowbel, D. et al. (2014) Transcriptional interference by antisense RNA is required for circadian clock function. *Nature*, 514, 650–653.
- Yamashita, A., Shichino, Y. & Yamamoto, M. (2016) The long non-coding RNA world in yeasts. *Biochimica et Biophysica Acta*, 1859, 147–154.
- Yang, X., Cui, H., Cheng, J., Xie, J., Jiang, D., Hsiang, T. et al. (2016) A HOPS protein, CmVps39, is required for vacuolar morphology, autophagy, growth, conidiogenesis and mycoparasitic functions of *Coniothyrium minitans*. *Environmental Microbiology*, 18, 3785–3797.
- Yen, M.R., Chen, J.S., Marquez, J.L., Sun, E.I. & Saier, M.H. (2010) Multidrug resistance: phylogenetic characterization of superfamilies of secondary carriers that include drug exporters. *Methods in Molecular Biology*, 637, 47–64.
- Yin, Y., Yan, P., Lu, J., Song, G., Zhu, Y., Li, Z. et al. (2015) Opposing roles for the lncRNA *haunt* and its genomic locus in regulating *HOXA* gene activation during embryonic stem cell differentiation. *Cell Stem Cell*, 16, 504–516.
- Yu, Y., Jiang, D., Xie, J., Cheng, J., Li, G., Yi, X. et al. (2012) Ss-Sl2, a novel cell wall protein with PAN modules, is essential for sclerotial development and cellular integrity of *Sclerotinia sclerotiorum*. *PLoS One*, 7, e34962.
- Yun, Y., Liu, Z., Yin, Y., Jiang, J., Chen, Y., Xu, J.R. et al. (2015) Functional analysis of the *Fusarium graminearum* phosphatome. *New Phytologist*, 207, 119–134.
- Zeng, W., Wang, J., Wang, Y., Lin, J., Fu, Y., Xie, J. et al. (2018) Dicer-like proteins regulate sexual development via the biogenesis of perithecial-specific microRNAs in a plant pathogenic fungus *Fusarium graminearum*. *Frontiers in Microbiology*, 9, 818.
- Zhang, L., Li, B., Zhang, Y., Jia, X. & Zhou, M. (2016) Hexokinase plays a critical role in deoxynivalenol (DON) production and fungal development in *Fusarium graminearum*. *Molecular Plant Pathology*, 17, 16–28.
- Zhou, X., Heyer, C., Choi, Y.E., Mehrabi, R. & Xu, J.R. (2010) The *CID1* cyclin C-like gene is important for plant infection in *Fusarium graminearum*. *Fungal Genetics and Biology*, 47, 143–151.
- Zhu, W., Wei, W., Fu, Y., Cheng, J., Xie, J., Li, G. et al. (2013) A secretory protein of necrotrophic fungus *Sclerotinia sclerotiorum* that suppresses host resistance. *PLoS One*, 8, e53901.

SUPPORTING INFORMATION

Additional supporting information may be found in the online version of the article at the publisher's website.

How to cite this article: Wang, J., Zeng, W., Cheng, J., Xie, J., Fu, Y., Jiang, D. et al. (2022) *lncRsp1*, a long noncoding RNA, influences *Fgsp1* expression and sexual reproduction in *Fusarium graminearum*. *Molecular Plant Pathology*, 23, 265–277. <https://doi.org/10.1111/mpp.13160>